J|A|C|S
COMMUNICATIONS

Published on Web 05/16/2007

Smart Aptamers Facilitate Multi-Probe Affinity Analysis of Proteins with Ultra-Wide Dynamic Range of Measured Concentrations

Andrei P. Drabovich, Victor Okhonin, Maxim Berezovski, and Sergey N. Krylov*

Department of Chemistry, York University, Toronto, Ontario M3J 1P3, Canada

Received April 1, 2007; E-mail: skrylov@yorku.ca

Protein concentrations can vary over several orders of magnitude in many physiological and pathological processes.[1] Studies of these processes require affinity analysis of proteins with a very wide dynamic range of accurately measured concentrations. Such an analysis can be realized with multiple affinity probes that bind the target with significantly different equilibrium constants (K_d).[2] Every probe in a multi-probe affinity analysis is responsible for detection of the target in the range of concentrations around its K_d value. A multi-probe affinity analysis of proteins was out of practical reach due to the lack of high-selectivity affinity probes with a wide range of K_d values.[3] Kinetic capillary electrophoresis (KCE) has been recently proven to generate "smart" DNA aptamers with high selectivity and a wide range of predefined K_d values.[4] Here, we demonstrate that such aptamers can facilitate multi-probe affinity analysis of a protein with an ultra-wide dynamic range of measured concentrations. In this proof-of-principle work, we used smart aptamers for MutS protein with K_d values of 7.6, 46, and 810 nM. MutS protein is an important and intensively studied player of the DNA repair machinery. Our results showed that the three-aptamer analysis of MutS had a concentration dynamic range of more than 4 orders of magnitude with an accuracy of 11%. To the best of our knowledge, this is the widest dynamic range ever reported for affinity analyses of proteins. This work proves that the wide range of predefined binding parameters of smart aptamers can bring new capabilities to quantitative affinity analyses. The same feature of smart aptamers makes them potentially indispensable molecular tools in studies of intracellular processes.

In a generic affinity analysis, a spectroscopically visible affinity probe P of known concentration $[P]_0$ is reacted with a spectroscopically invisible target T of unknown concentration $[T]_0$, which is to be determined. P binds T and forms a detectable target−probe complex T·P at equilibrium

$$T + P \rightleftarrows T{\cdot}P, \quad K_d = [T][P]/[T{\cdot}P] \tag{1}$$

where [T], [P], and [T·P] are equilibrium concentrations of T, P, and T·P, respectively. The free probe is separated from the target−probe complex physically or spectrally to find fraction f of the bound probe in the equilibrium mixture: $f = [T{\cdot}P]/[P]_0$. Finally, the unknown concentration of target is calculated

$$[T]_0 = ([P]_0 + K_d/(1 - f))\, f \tag{2}$$

In a general case, when a mixture of n ($n \geq 1$) probes is used, eq 2 converts into the following (see Supporting Information):

$$\sum_{i=1}^{n} \frac{[P]_{0_i}}{K_{d_i} + [T]_0 - f\sum_{j=1}^{n}[P]_{0_j}} = \frac{f\sum_{i=1}^{n}[P]_{0_i}}{[T]_0 - f\sum_{i=1}^{n}[P]_{0_i}} \tag{3}$$

where K_{d_i} and $[P]_{0_i}$ are the parameters of probe i ($i = 1, ..., n$).

Binding curves f versus $[T]_0$, which are obtained from eq 3, visualize the dynamic range of the analysis (Figure 1). The concentration dynamic range is the region of $[T]_0$ where the binding curve has a slope sufficiently steep to find $[T]_0$ with a required accuracy. When a single probe is used in an affinity analysis, the dynamic range lies around its K_d value and typically covers only 1−2 orders of magnitude. The dynamic range can be greatly extended if more than one probe with significantly different K_d values is used (Figure 1). The probes can be used individually in separate analyses to achieve the greatest extension (Figure 1A). Alternatively, they can be used as a mixture in a single analysis with still a very wide dynamic range and an advantage of simplicity (Figure 1B). To have a dynamic range of 4 orders of magnitude, the multi-probe analysis has to employ affinity probes with K_d values in a range of at least 2 orders of magnitude (the difference in K_d between "adjacent" probes should not significantly exceed 1 order of magnitude to avoid blind areas on the binding curve; see Supporting Information). Obtaining antibodies with a K_d range of 2 orders of magnitude is virtually impossible without compromising their selectivity. We have recently proven that DNA aptamers provide a vital alternative.[4]

Aptamers are selected in a process termed SELEX.[5] The conventional SELEX typically requires more than 10 rounds of selection and leads to very few unique aptamers with binding parameters in a narrow and hardly predictable range. Selection of smart aptamers by methods of KCE overcomes the limitations of conventional SELEX: the number of required rounds is typically below five, and a large number of unique aptamers can be selected with binding parameters predefined in a wide range.[4]

In our recent work, we used KCE to select smart DNA aptamers for MutS protein with predefined K_d values in a range of over 2 orders of magnitude.[4b,c] Here we employed three of those aptamers with K_d values of 7.6, 46, and 810 nM to develop the first aptamer-based multi-probe affinity analysis. The generic procedure for an affinity analysis described above was used with the following specifics. The aptamers were fluorescently labeled for sensitive detection. The individual aptamers or an equimolar mixture of them was reacted with MutS to reach equilibrium. The aptamer−protein complexes were separated from free aptamers by a KCE method known as nonequilibrium capillary electrophoresis of equilibrium mixtures (NECEEM).[6] The fraction of the bound aptamer was calculated from the areas of peaks in a NECEEM electropherogram as explained in Figure 2.

Using this approach, we built binding curves f versus $[T]_0$ for the three individual aptamers (Figure 3A) and for their equimolar mixture (Figure 3B). All experiments were done in triplicate, and their results are shown as points. Theoretical binding curves were calculated using eq 3; they are shown as solid lines. Importantly, the theoretical curves fit perfectly the experimental data. This suggests that aptamers bind MutS with 1:1 stoichiometry, and no

 10.1021/ja072269p CCC: $37.00

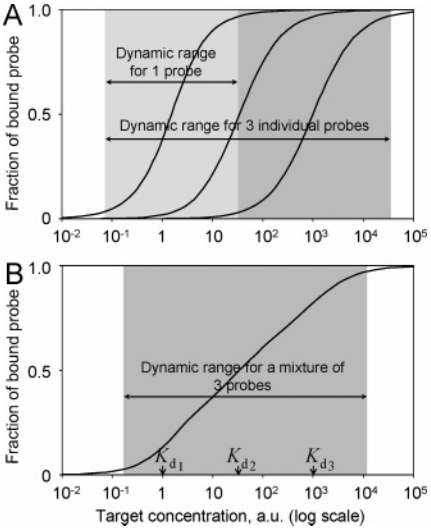

Figure 1. Schematic representation of the dynamic range extension for affinity analysis using three individual affinity probes with K_d values of 1, 33, and 1000 au and a concentration of 1 au (A) and a mixture of these probes at concentrations of 1 au each (B). The binding curves were calculated using eq 3 with $n = 1$ (panel A) and $n = 3$ (panel B).

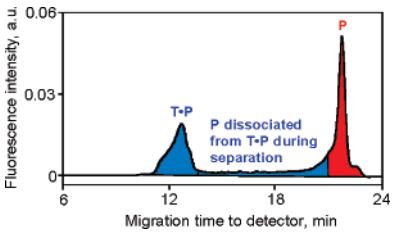

Figure 2. Determination of the fraction f of bound aptamer in aptamer-based affinity analysis of MutS protein using the NECEEM method. The blue and red areas in the electropherogram represent the amounts of bound and unbound aptamer, respectively, in the equilibrium mixture. The fraction of bound aptamer is calculated as a ratio between the blue and the sum of the blue and red areas corrected for migration times of corresponding species (see Supporting Information).

interference occurs between the aptamers in the mixture. It also suggests that building the calibration curves for the affinity analysis is not necessary; eq 3 can be directly utilized for finding unknown $[T]_0$ using known K_d, f, and $[P]_0$. The concentration dynamic ranges for affinity analyses were defined for 11% accuracy of protein concentration determination. The dynamic range for a single-probe analysis was approximately 2 orders of magnitude. The three individual probes covered the overall dynamic range of 5 orders of magnitude. The analysis based on a mixture of the three probes had a dynamic range of more than 4 orders of magnitude with a limit of detection of 0.1 nM of $[MutS]_0$. These results prove that smart aptamers can facilitate multi-probe affinity analysis of proteins with an ultra-wide dynamic range. Moreover, the three-aptamer analysis of MutS developed here can be directly used in studying cellular DNA repair machinery.

We then tested the selectivity of the aptamer-based multi-probe affinity analysis of MutS. Different concentrations of MutS (0.18 μg to 0.18 mg in mL) were detected in the presence of 2.5% fetal bovine serum (FBS), which contained 1.1 mg/mL of total protein. MutS in the presence of FBS was measured using the mixture of the three aptamers. The results of such analyses (Figure 3B, black squares) showed no significant difference from those of the analyses of MutS in a bare buffer. The tolerance of the analysis to the presence of other proteins suggests its potential utility in applications ranging from basic research to clinical analyses.

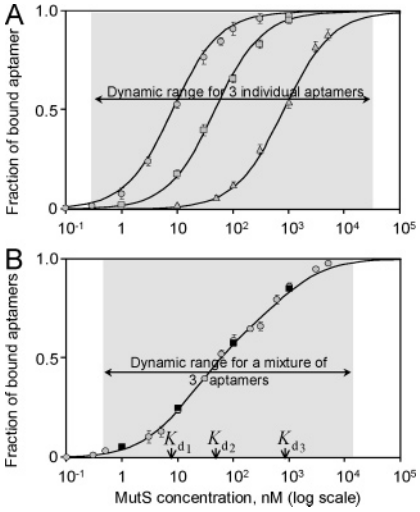

Figure 3. Concentration dynamic range for the affinity analysis of MutS protein using 1 nM of three individual aptamers with K_d values of 7.6, 46, and 810 nM (A), and a mixture of 1 nM of these aptamers (B). Solid lines were calculated with eq 3 using the above values of K_d and concentrations. Gray points correspond to analyses of MutS in the bare buffer (50 mM Tris-acetate, pH 8.2), while black squares correspond to analyses of MutS in the presence of 2.5% FBS in the buffer.

Finally, we outline the major features of the multi-aptamer affinity analysis of protein. The use of multiple aptamers extends the concentration dynamic range to more than 2 orders of magnitude plus the range of K_d values of the aptamers used. Advantageously, the concentration of the target can be found with a simple calibration-free approach. When the target is present in a complex biological matrix, protecting aptamers from nucleases can be required. If the sample matrix contains DNA-binding proteins, their nonspecific binding to aptamers can be suppressed by adding the excess of nonlabeled scrambled DNA.

To conclude, this work proves that unique features of smart ligands can significantly extend capabilities of quantitative affinity analyses. The particular analysis developed here is being productively used in studies of MutS protein, an important player in the DNA repair machinery. We foresee new enabling applications of smart ligands in analyses and therapies that require well-defined dynamics of target−ligand interaction.

Acknowledgment. The work was funded by NSERC Canada.

Supporting Information Available: Supporting materials and methods and complete ref 3 (PDF). This material is available free of charge via the Internet at http://pubs.acs.org.

References

(1) (a) Moll, D.; Prinz, A.; Gesellchen, F.; Drewianka, S.; Zimmermann, B.; Herberg, F. W. *J. Neural Transm.* **2006**, *113*, 1015−1032. (b) Wilson, D. W. *Science* **2002**, *295*, 2103−2105. (c) Yamaguchi, H.; Yoshida, J.; Yamamoto, K.; Sakata, Y.; Mano, T.; Akehi, N.; Hori, M.; Lim, Y.-J.; Mishima, M.; Masuyama, T. *J. Am. Coll. Cardiol.* **2004**, *43*, 55−60.
(2) Marvin, J. S.; Corcoran, E. E.; Hattangadi, N. A.; Zhang, J. V.; Gere, S. A.; Hellinga, H. W. *Proc. Natl. Acad. Sci. U.S.A.* **1997**, *94*, 4366−4371.
(3) Taussig, M. J.; et al. *Nat. Methods* **2007**, *4*, 13−17.
(4) (a) Petrov, A.; Okhonin, V.; Berezovski, M.; Krylov, S. N. *J. Am. Chem. Soc.* **2005**, *127*, 17104−17110. (b) Drabovich, A.; Berezovski, M.; Krylov, S. N. *J. Am. Chem. Soc.* **2005**, *127*, 11224−11225. (c) Drabovich, A. P.; Berezovski, M.; Okhonin, V.; Krylov, S. N. *Anal. Chem.* **2006**, *78*, 3171−3178. (d) Berezovski, M.; Musheev, M.; Drabovich, A.; Krylov, S. N. *J. Am. Chem. Soc.* **2006**, *128*, 1410−1411. (e) Berezovski, M.; Musheev, M. U.; Drabovich, A. P.; Jitkova, J.; Krylov, S. N. *Nat. Protoc.* **2006**, *1*, 1359−1369.
(5) (a) Tuerk, C.; Gold, L. *Science* **1990**, *249*, 505−510. (b) Mendonsa, S. D.; Bowser, M. T. *J. Am. Chem. Soc.* **2004**, *126*, 20−21.
(6) Berezovski, M.; Krylov, S. N. *J. Am. Chem. Soc.* **2002**, *124*, 13674−13675.

JA072269P

SUPPORTING INFORMATION

Smart Aptamers Facilitate Multi-Probe Affinity Analysis of Proteins with Ultra-Wide Dynamic Range of Measured Concentrations

Andrei P. Drabovich, Victor Okhonin, Maxim Berezovski, and Sergey N. Krylov

Department of Chemistry, York University, Toronto, Ontario, Canada M3J 1P3

1. Supporting Materials and Methods

Materials. A biotin-labeled primer, a fluorescein-labeled primer, and non-labeled synthetic aptamers were obtained from IDT (Coralville, IA, USA). Recombinant *Taq* DNA polymerase, EGTA, and all other chemicals were from Sigma-Aldrich (Oakville, ON, Canada) unless otherwise stated. Thermostable DNA mismatch binding protein (MutS) from *Thermus aquaticus* was purchased from InterSciences (Markham, ON, Canada). A fused-silica capillary was purchased from Polymicro (Phoenix, AZ, USA). All solutions were made using Milli-Q-quality deionized water filtered through a 0.22 μm filter (Millipore, Nepean, ON). Streptavidin-coated paramagnetic beads (Dynabeads M-280 Streptavidin) were obtained from Invitrogen. Standard fetal bovine serum (SH30397.03) was purchased from HyClone (Logan, UT, USA).

Preparation of fluorescently labeled aptamers and their properties. The following fluorescently labeled aptamers were obtained by PCR amplification of corresponding non-labeled aptamers using fluorescein (FAM)- and biotin-labeled primes as described below:

Sequence (5'→3')	K_d, nM
FAM-CTTCTGCCCGCCTCCTTCC**GTCTTATGTCGTTAGTCGCAGGGTGATGAGTGAGGCAAG**GGAGACGAGATAGGCGGACACT	7.6
FAM-CTTCTGCCCGCCTCCTTCC**CTAGTGCAGGGGTTCACTCAGGACCTTACGAGCTTTTTC**GGAGACGAGATAGGCGGACACT	46
FAM-CTTCTGCCCGCCTCCTTCC**CGCACTTGCAAACCTTCATGGTCTCGTGCTTGAGTGGTT**GGAGACGAGATAGGCGGACACT	810

Non-labeled synthetic aptamer sequences were amplified by PCR in 25 cycles with 300 nM reverse 5'-biotin-labeled and forward 5'-FAM-labeled primers. The obtained double-stranded DNA was mixed with streptavidin-coated paramagnetic beads, and the strands were separated as described elsewhere.[S1] In essence, single-stranded 5'-FAM-labeled aptamers were eluted from paramagnetic beads and collected, while 5'-biotin-labeled complimentary strands remained attached to the beads and were discarded. Aptamers were concentrated using ethanol precipitation and dissolved in 50 mM Tris-Acetate at pH 8.2. Stock solutions of aptamers had concentrations of 121 nM, 91 nM, and 87 nM, respectively. The three aptamers were used for multi-probe affinity analyses of MutS.

The most thermodynamically stable stem-loop structures of the three aptamers are shown in **Fig. S1**. MutS natively binds single-nucleotide mismatches in double stranded DNA.[S2,S3] The structures of the aptamers have no single-nucleotide mismatches, which indicates, that the nature of aptamer affinity to MutS is different from that of single-nucleotide mismatches. Different natures of aptamer and mismatch binding to MutS lead to different K_d values. The lowest K_d for MutS binding to a mismatch is 120 nM for the G-T mismatch; the value of K_d increases up to 2.7

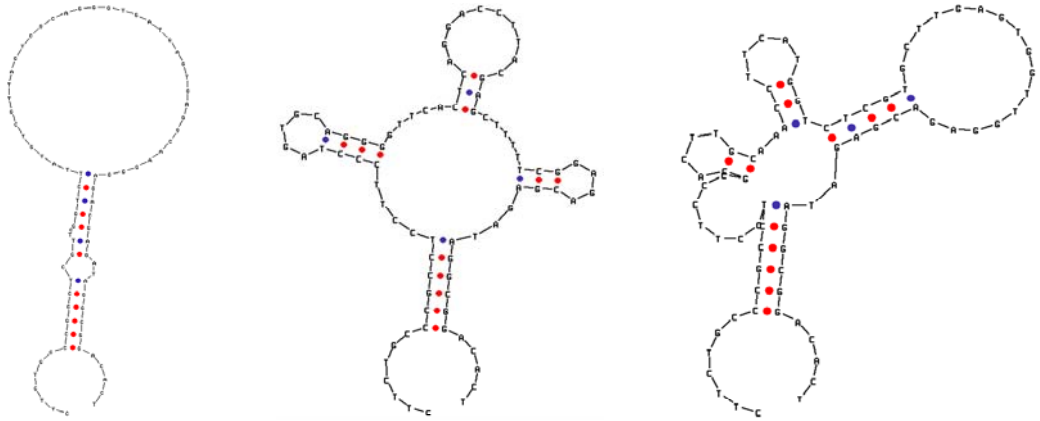

Figure S1. Stem-loop structures of smart aptamers and their respective affinities to *Taq* MutS protein.

μM for a perfectly matched double-stranded DNA (unpublished data). The K_d value of MutS binding to a random 80-nt DNA library is 2.1 μM, while that of MutS binding to a single-stranded DNA with no secondary structure was estimated to be higher than 300 μM.[S4] The majority of the selected aptamers have K_d values considerably lower than those of mismatched or other DNA structures.

Mismatch binding to MutS is suppressed in the absence of 2-5 mM magnesium ions, while binding of aptamers to MutS is not sensitive to magnesium.[S2,S3] Mismatches bind MutS of different species with similar affinities, while aptamers do not. For example, an aptamer, which was selected for *Taq* MutS and can bind *Taq* MutS with K_d = 7.6 nM, binds *E. coli* MutS with K_d = 590 nM (unpublished data). Thus, the aptamers are not only very tight binders but also highly selective binders.

Determination of *f* and K_d using NECEEM. All MutS-aptamer equilibrium mixtures for NECEEM measurements were prepared in 50 mM Tris-Acetate buffer at pH 8.2 using the following two-step procedure. First, 4 μL of the 2 nM solution of FAM-labeled DNA aptamer (or a mixture of the three aptamers, each at a concentration of 2 nM) in the Tris-Acetate buffer was denatured by heating at 80 °C for 2 min with subsequent cooling down to 15 °C at a rate of 7.5 deg/min. Second, 4 μL of the MutS solution in the Tris-Acetate was mixed with the DNA sample and incubated at 15 °C for 30 min to obtain the equilibrium mixture.

A plug of the equilibrium mixture was injected into the capillary and subjected to non-equilibrium capillary electrophoresis of equilibrium mixtures (NECEEM) at 375 V/cm and 15 °C. The Tris-Acetate used for the preparation of the equilibrium mixture was also used as a run buffer in gel-free electrophoresis. An 80-cm long fused-silica capillary (70 cm from the injection end to the detection window) with a 150 μm inner diameter was used in all experiments.

In the following consideration, a protein is called a target (T) and an aptamer is called a probe (P). The equilibrium dissociation constant, K_d, of target-probe complex (T·P) was found from a standard Scatchard plot using experimentally determined fractions *f* of the bound probe. The value of *f* was calculated from the NECEEM electropherogram using peak areas of the complex ($A_{T\cdot P}$), the probe dissociated from the complex during separation ($A_{P\ dissociated}$), and the free probe (A_P) from the following equation:

$$f = \frac{A_{T\cdot P}/t_{T\cdot P} + A_{P\ dissociated}/t_P}{A_P/t_P + A_{T\cdot P}/t_{T\cdot P} + A_{P\ dissociated}/t_P} \quad \text{(S1)}$$

The peak areas in equation S1 were divided by migration times of the corresponding species ($t_{T\bullet P}$ for the complex and t_P for the probe) to correct for differences in the residence time of T·P and P in the detection window induced by differences of their velocities.

Combination of multiple probes in the analysis. Here we present the derivation of an equation for the calculation of $[T]_0$ for the case when a mixture of three probes is used in the affinity analysis. When three probes (P_1, P_2 and P_3) with different K_d values are used to detect one target, three equilibria are simultaneously established in the equilibrium mixture:

$$\begin{cases} T + P_1 \rightleftarrows T\bullet P_1 \\ T + P_2 \rightleftarrows T\bullet P_2 \\ T + P_3 \rightleftarrows T\bullet P_3 \end{cases} \quad \text{(S2)}$$

The three equilibria are described by:

a) A set of equilibrium dissociation constants:

$$\begin{cases} K_{d_1} = [T][P]_1/[T\bullet P]_1 \\ K_{d_2} = [T][P]_2/[T\bullet P]_2 \\ K_{d_3} = [T][P]_3/[T\bullet P]_3 \end{cases} \quad \text{(S3)}$$

b) Mass balances for the three probes:

$$\begin{cases} [P]_{0_1} = [P]_1 + [T\bullet P]_1 \\ [P]_{0_2} = [P]_2 + [T\bullet P]_2 \\ [P]_{0_3} = [P]_3 + [T\bullet P]_3 \end{cases} \quad \text{(S4)}$$

and

c) Mass balance for the target:

$$[T]_0 = [T] + [T\bullet P]_1 + [T\bullet P]_2 + [T\bullet P]_3 \quad \text{(S5)}$$

Since DNA aptamers (probes) have identical lengths, they migrate with the same velocity in gel-free electrophoresis. Protein-aptamer (target-probe) complexes have identical velocities as well. As a result, we can determine a collective fraction f of bound aptamers using sum concentrations of probes and complexes:

$$f = \frac{[T\bullet P]_1 + [T\bullet P]_2 + [T\bullet P]_3}{[P]_{0_1} + [P]_{0_2} + [P]_{0_3}} \quad \text{(S6)}$$

Combining Eqs. S2-S6, we get an equation which links the unknown total concentration of the target $[T]_0$ with known f, $[P]_{0_1}$, $[P]_{0_2}$, $[P]_{0_3}$, K_{d_1}, K_{d_2}, and K_{d_3}:

$$\frac{[P]_{0_1}}{K_{d_1} + [T]_0 - f\times([P]_{0_1} + [P]_{0_2} + [P]_{0_3})} + \frac{[P]_{0_2}}{K_{d_2} + [T]_0 - f\times([P]_{0_1} + [P]_{0_2} + [P]_{0_3})} + \\ + \frac{[P]_{0_3}}{K_{d_3} + [T]_0 - f\times([P]_{0_1} + [P]_{0_2} + [P]_{0_3})} = \frac{f\cdot([P]_{0_1} + [P]_{0_2} + [P]_{0_3})}{[T]_0 - f\times([P]_{0_1} + [P]_{0_2} + [P]_{0_3})} \quad \text{(S7)}$$

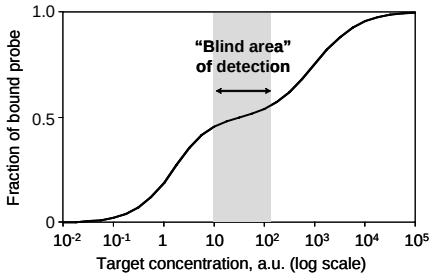

Figure S2. Schematic representation of a "blind area" on the titration curve using a mixture of two affinity probes with K_d values of 1 and 1000 a.u. and a concentration of 1 a.u. The binding curve was calculated using Eq. S8 for $n = 2$.

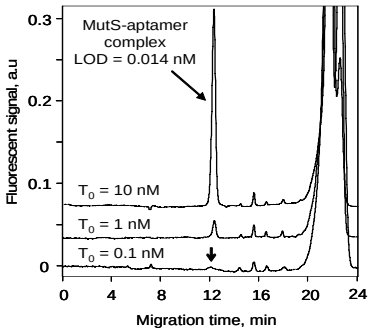

Figure S3. Limit of detection of NECEEM-based affinity analysis. Electropherograms show the analysis of 10 nM, 1 nM and 0.1 nM MutS protein using a combination of three aptamers.

In a general case, when a mixture of n ($n \geq 1$) probes is used, Eq. S7 converts into the following expression:

$$\sum_{i=1}^{n} \frac{[\mathrm{P}]_{0_i}}{K_{\mathrm{d}_i} + [\mathrm{T}]_0 - f \cdot \sum_{j=1}^{n} [\mathrm{P}]_{0_j}} = \frac{f \cdot \sum_{i=1}^{n} [\mathrm{P}]_{0_i}}{[\mathrm{T}]_0 - f \cdot \sum_{i=1}^{n} [\mathrm{P}]_{0_i}} \qquad \text{(S8)}$$

where K_{d_i} and $[\mathrm{P}]_{0_i}$ are the parameters of the "i"-th probe ($i = 1,\ldots, n$). Eq. S8 can be solved for $[\mathrm{T}]_0$ with an Excel solver (or another solver of algebraic equations) to calculate the unknown target concentration $[\mathrm{T}]_0$.

"Blind areas" in multiple-probe analysis. A "blind area" is a plateau on the binding curve where the steepness of the curve is not sufficient to provide high-accuracy determination of target concentration (**Fig. S2**). A blind area is caused by a significant difference in K_d of the adjacent probes (similar plateaus are observed during titration of polyprotic acids). To avoid blind areas, the difference in K_d values of the adjacent probes should not significantly exceed one order of magnitude. Smart aptamers are excellent affinity probes for this type of analyses as they can be selected with desired K_d values to ensure K_d of adjacent aptamers are properly spaced.

The limit of detection of NECEEM-based affinity analysis. CE with laser-induced fluorescence detection facilitates highly sensitive quantitation of fluorescently labeled molecules. The mass limit of detection of CE is superb but due to small injection volumes the concentration detection limit is relatively poor. To improve the concentration limit of detection, an 80-cm long capillary with a 150 μm inner diameter was used for the analysis. In addition, the choice of the CE run buffer (50 mM Tris-Aceate at pH 8.2) also contributed to the improved limit of detection. The run buffer facilitated very good separation of MutS-aptamer complexes from the excess of free aptamers (**Fig. S3**) and generated very low electrical current, thus, allowing us to use a wide capillary without decreasing the electric field. Due to these optimizations, we were able to inject a plug of 235 nL and detect subnanomolar concentrations of aptamers and MutS-aptamer complexes. The limit of detection of MutS-aptamer complexes that did not dissociate during the separation was estimated to be 0.014 nM at S/N = 3. As a result, 0.1 nM concentration of total MutS in the equilibrium mixture was detected (**Fig. S3**).

Analysis of MutS in the presence of fetal bovine serum (FBS). The analysis of MutS in the presence of 2.5% FBS required additional optimization to suppress the degradation of DNA aptamers by nucleases and the binding of aptamers by DNA-binding proteins that might be present in FBS. EGTA at a final concentration of 10 mM was used to suppress the activity of nucleases and metallo-proteases,[S5,S6] while 10 μM unlabeled scrambled DNA was added to

eliminate non-specific binding of aptamers by DNA-binding proteins. These reagents did not interfere with MutS-aptamer interaction; however, their absence in the equilibrium mixture resulted in rapid aptamer degradation and pronounced non-specific binding of aptamers by DNA-binding proteins.

Equilibrium mixtures were prepared in 50 mM Tris-Acetate buffer at pH 8.2 using the following two-step procedure. First, 0.8 μL of a mixture of three fluorescently labeled aptamers (10 nM each) was dissolved in 4 μL of the Tris-Acetate buffer and denatured by heating at 80 °C for 2 min with subsequent cooling down to 15 °C at a rate of 7.5 deg/min. Then, the following components were added: 0.8 μL of 100 mM EGTA-Na at pH 8.0, 0.8 μL of 100 μM unlabeled DNA (5'-CTC CTC TGA CTG TAA CCA CG-3'), 0.8 μL of MutS protein (at one of the following concentrations: 10 or 1 μM, or 100 or 10 nM), 0.8 μL of FBS diluted 4 times in the Tris-Acetate buffer (undiluted FBS had 45 mg/mL of total protein). The mixtures were incubated at 15 °C for 30 min to reach the equilibrium and analyzed with NECEEM as described above.

References

S1. Berezovski, M.; Musheev, M.U.; Drabovich, A.P.; Jitkova, J.; Krylov, S.N. *Nature Protoc.* **2006**, *1*, 1359-1369.
S2. Drabovich, A.P.; Krylov, S.N. *Analytical Chemistry* **2006**, *78*, 2035-2038.
S3. Biswas, I.; Hsieh, P. *J.Biol.Chem.* **1996**, *271*, 5040-5048.
S4. Drabovich, A.; Berezovski, M.; Krylov, S. N., *J. Am. Chem. Soc.* **2005**, *127*, 11224–11225.
S5. Liu, D.; Wu, R. *BioTechniques* **1999**, *26*, 258-261.
S6. Gegenheimer, P. *Methods Enzymol.* **1990**, *182*, 174-193.

2. Full Reference 3

Taussig, M.J.; Stoevesandt, O.; Borrebaeck, C.A.K.; Bradbury, A.R.; Cahill, D.; Cambillau, C.; de Daruvar, A.; Dübel, S.; Eichler, J.; Frank, R.; Gibson, T.J.; Gloriam, D.; Gold, L.; Herberg, F.W.; Hermjakob, H.; Hoheisel, J.D.; Joos, T.O.; Kallioniemi, O.; Koegl, M.; Konthur, Z.; Korn, B.; Kremmer, E.; Krobitsch, S.; Landegren, U.; van der Maarel, S.; McCafferty, J.; Muyldermans, S.; Nygren, P.-Å.; Palcy, S.; Plückthun, A.; Polic, B.; Przybylski, M.; Saviranta, P.; Sawyer, A.; Sherman, D.J.; Skerra, AS.; Templin, M.; Ueffing, M.; Uhlén, M. *Nat. Methods* **2007**, *4*, 13-17.